Modification of a Na-montmorillonite with quaternary ammonium salts and its application for organics removal from TNT red water

Qian Zhang, Zilin Meng, Yihe Zhang, Guocheng Lv, Fengzhu Lv and Limei Wu

ABSTRACT

Na-montmorillonite (Na-Mont) and organic montmorillonite modified by cetyltrimethylammonium bromide (CTAB-Mont) and tetramethylammonium bromide (TMAB-Mont) were prepared as adsorbents to remove organic contaminants from 2,4,6-trinitrotoluene (TNT) red water. The characterizations of the samples were performed with X-ray diffraction and Fourier transform infrared spectroscopy. The adsorption capacity of CTAB-Mont (15.9 mg/g) was much larger than Na-Mont (0.26 mg/g) and TMAB-Mont (1.7 mg/g). Langmuir isotherm and the pseudo-second-order kinetic models fitted the experimental results well. The main factor in the adsorption promotion was the distribution phase in the interlayer of CTAB-Mont. The arrangement of molecules analyzed by molecular simulation corresponded to the experimental data and supported the adsorption mechanism.

Key words | adsorption, conformation, intercalation, montmorillonite, TNT red water

Qian Zhang
Zilin Meng
Yihe Zhang (corresponding author)
Guocheng Lv
Fengzhu Lv
Limei Wu
National Laboratory of Mineral Materials,
School of Materials Science and Technology,
China University of Geosciences,
Beijing, 100083,
China
E-mail: *zyh@cugb.edu.cn*

INTRODUCTION

2,4,6-Trinitrotoluene (TNT) as an explosive has been widely used for military and civilian purpose. Large amounts of waste water are generated during the manufacturing and refining of TNT, which is carcinogenic, toxic, mutagenic, and hardly biodegradable (Nefso *et al.* 2005). TNT red water discharged without any effective treatment will contaminate water and soil, causing serious environmental problems. Several methods are used to remove organic contaminants from TNT red water, such as adsorption (Nehrenheim *et al.* 2011; Wei *et al.* 2011), biological methods (Maloney *et al.* 2002), catalytic destruction (Schmelling & Gray 1995) and degradation (Davel *et al.* 2003).

Na-montmorillonite (Na-Mont) has a 2:1 configuration consisting of two silicon–oxygen tetrahedral sheets and one aluminum–oxygen–hydroxyl octahedral sheet. Due to its large surface area and high cation-exchange capacity, Na-Mont, which has no adsorption capacity for anionic contaminants, is widely used as an adsorbent to remove cationic contaminants (Zhou *et al.* 2013). Na^+ in the interlayer of Na-Mont can be readily replaced by quaternary ammonium organic cations (QACs) to enhance the adsorption capacity of the host towards organic contaminants (Liu *et al.* 2012). But few reports on the treatment of organics from TNT red water by modified Na-Mont have been published. In the present study the Na-Mont was modified using cetyltrimethylammonium bromide (CTAB) and tetramethylammonium bromide (TMAB) and the adsorption efficiency of the modified samples was evaluated. The adsorption mechanism, interlayer anionic organic distribution, and the arrangement of the molecules were analyzed.

MATERIALS AND METHODS

Materials

Na-Mont powder was supplied from Zhejiang, China. CTAB ($C_4H_{12}BrN$) and TMAB ($C_{19}H_{42}BrN$) were purchased from Beijing Chemical Plant. The TNT red water was provided by Dongfang Chemical Corporation (Hubei, China). The main organic contaminants in TNT red water were 2,4-dinitrotoluene-3-sulfonate and 2,4-dinitrotoluene-5-sulfonate (DNT-sulfonate), which occupied more than 91%, and the

doi: 10.2166/wst.2014.039

chemical oxygen demand (COD) of TNT red water diluted 100 times was 850 ± 20 mg/L (Fu *et al.* 2012).

Modification of Na-Mont

The CTAB solution (6.00 g in 100 mL) or TMAB solution (2.54 g in 100 mL) was slowly added to the Na-Mont dispersion (10 g in 300 mL) and the mixture was incubated at 60 °C for 10 h under slight stirring. Then, the suspension was filtered, and washed repeatedly until it was free of Br^-. Finally, CTAB-Mont and TMAB-Mont were dried at 80 °C and ground to 100 mesh.

Batch treatment of TNT red water

Batch adsorption experiments were conducted using 0.4 g of adsorbents in 25 mL of TNT red water. The thermodynamics and kinetics were studied using TNT red water with different concentrations (COD from 200 to 2,000 mg/L). CTAB-Mont after adsorption was assigned as CTAB-Mont-X, where X was the initial COD of red water. The filtrate was analyzed by a COD rapid detector (5B-3C, Lian-Hua Tech. Co., China). Each experiment was repeated twice and the average value is presented.

The amount of COD adsorbed (mg/g) by adsorbents can be calculated as follows:

$$q_e = \frac{(c_0 - c_e)V}{W}$$

where q_e is the amount adsorbed per unit mass of adsorbent at equilibrium (mg/g), c_0 and c_e (mg/L) are the COD of initial TNT red water and after adsorption equilibrium respectively, W (g) is the absorbent weight and V (L) is the volume of TNT red water.

Characterization

Fourier transform infrared spectroscopy (FT-IR) spectra were acquired from KBr disks on a Perkin Elmer spectrum 100 FT-IR spectrophotometer (Perkin Elmer, USA). X-ray diffraction (XRD) patterns of the prepared samples were obtained on a D/MAX-RC diffractometer (Rigaku, Japan) using CuK_α radiation (40 kV, 100 mA). The Materials Studio 5.0 was used to perform molecular simulation in order to investigate the adsorption and molecule conformation in the interlayer of Na-Mont. The formula of Na-Mont is $Na_{0.625}Si_8(Al_{3.375}Mg_{0.625})O_{20}(OH)_4$ with a formula weight of 732.5 g/mol. The molecular simulation and established model were optimized. After the system reached equilibrium, the NVT kinetic simulation was performed under the same conditions (Wu *et al.* 2010; Lv *et al.* 2011).

RESULTS AND DISCUSSION

Adsorption kinetics

The adsorption dynamics describe the rate of adsorption, which expresses the residence time at the solid–solution interface. The pseudo-first-order and the pseudo-second-order models could be used to assess the adsorption of organic contaminants from TNT red water onto adsorbents (Limousin *et al.* 2007).

The pseudo-first-order model presents as the following form:

$$\frac{dq}{dt} = k_1(q_e - q)^2$$

where q (mg/g) is the amount of organic contaminants at any time. k_1 (min^{-1}) is the equilibrium rate constant and t (min) is the adsorption time.

The pseudo-second-order model presents as the following form:

$$\frac{dq}{dt} = k_2(q_e - q)^2$$

where k_2 (g/(mg · min)) is the equilibrium rate constant of pseudo-second-order sorption.

Figure 1 shows that Na-Mont had no adsorption capacity for organics in TNT red water, while the adsorption capacity

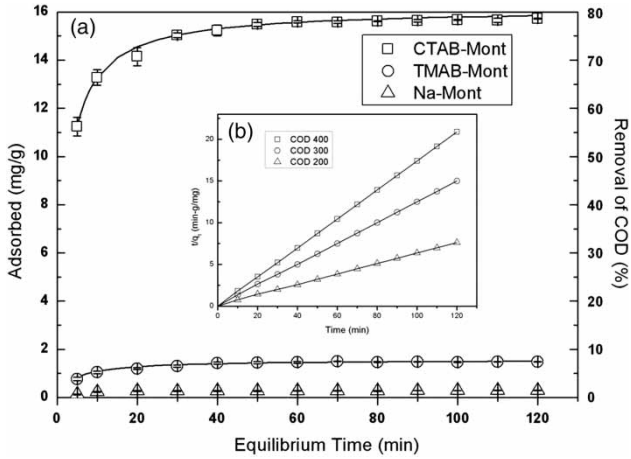

Figure 1 | (a) Kinetics of contaminant adsorption on Na-Mont (△), TMAB-Mont (○) and CTAB-Mont (□). The solid line is pseudo-second-order fit to the observed data. (b) Insert is plots of t/qt against t for CTAB-Mont at different initial COD.

of CTAB-Mont and TMAB-Mont increased rapidly in the first 20 min, and then increased steadily to reach equilibrium. After equilibrium the q_e of CTAB-Mont and TMAB-Mont were 15.9 and 1.7 mg/g respectively, while their COD removal rates were 79.1 and 8.5% respectively. In comparison with TMAB-Mont, the removal of COD and adsorption capacity of CTAB-Mont were much higher. In the present study, the correlation coefficient from the pseudo-second-order kinetic equation was high ($R^2 > 0.990$) at different initial concentrations (Figure 1(b)), and the calculated equilibrium adsorption capacity (16.5 mg/g) fits well with the experiment data (15.9 mg/g), whereas the correlation coefficient of the pseudo-first-order model was low ($R^2 < 0.905$). The R^2 and q_e value both demonstrated that the adsorption kinetics followed the pseudo-second-order model and the rate constant was calculated ($k_2 =$ 0.42 g/(mg·min)). The instantaneous removal of DNT-sulfonate by CTAB-Mont suggested a great affinity of the organic contaminants towards the organic phase in CTAB-Mont.

Adsorption isotherms

The adsorption isotherm is an efficient way to predict the modeling procedures of adsorption systems. The theoretical Langmuir isotherm (Limousin *et al.* 2007) is a monolayer adsorption and represented as follows:

$$q_e = \frac{Q_0 b C_e}{1 + bC_e}$$

where Q_0 is a Langmuir adsorption constant reflecting the maximum adsorption capacity (mg/g) and b is a constant (L/mg).

The separation factor is a dimensionless constant called equilibrium parameter (R_L), and it is defined to estimate the adsorption condition. The equation is given by:

$$R_L = \frac{1}{1 + bC_0}$$

The value of R_L has three possibilities: $0 < R_L < 1$ indicates a favorable adsorption, $R_L > 1$ indicates an unfavorable adsorption, and $R_L = 1$ indicates a linear adsorption.

The Freundlich isotherm assumes the surface heterogeneity and encompasses exponential distribution of the active sites and energies. The empirical Freundlich isotherm equation can be given by:

$$q_e = K_F C_e^{1/n}$$

where K_F ((mg/g) (L/mg)$^{1/n}$) and n (dimensionless) are the Freundlich constants which indicate the adsorption capacity and adsorption intensity respectively.

Figure 2 demonstrates that the adsorption capacity of TMAB-Mont was far lower than that of CTAB-Mont, indicating that CTAB in the Na-Mont played an important role. The Freundlich fit resulted in a big discrepancy between the observed and predicted date ($R^2 < 0.952$), and the Langmuir model had a better fit for both CTAB-Mont and TMAB-Mont ($R^2 > 0.997$). The better fit to the Langmuir model suggested a surface-limited adsorption. Q_0 for anionic organic contaminant adsorption on CTAB-Mont was calculated to be 33.4, 41.0 and 45.4 mg/g at 30, 40, 50 °C, respectively. The calculated values of R_L based on the Langmuir isotherm in the tested temperature was between 0.0999 and 0.5426, indicating that contaminant adsorption on CTAB-Mont was favorable.

FT-IR analysis

FT-IR spectra of the samples are shown in Figure 3. The characteristic peaks at 2,921 and 2,852 cm^{-1} belonged to the C–H antisymmetric stretching vibration and symmetric stretching vibration, respectively. The peak of 1,470 cm^{-1} was amino methylene groups in shear vibration. All these characteristic peaks above showed the QACs had been adsorbed into the interlayer. Otherwise, the characteristic absorption peak of amino methylene groups was shifting, and it was shown that the arrangement of QACs in the Na-Mont was transformed.

Compared with pure TMAB-Mont, TMAB-Mont after adsorption in the effluent remained unchanged. It meant that the contaminants could not be absorbed by

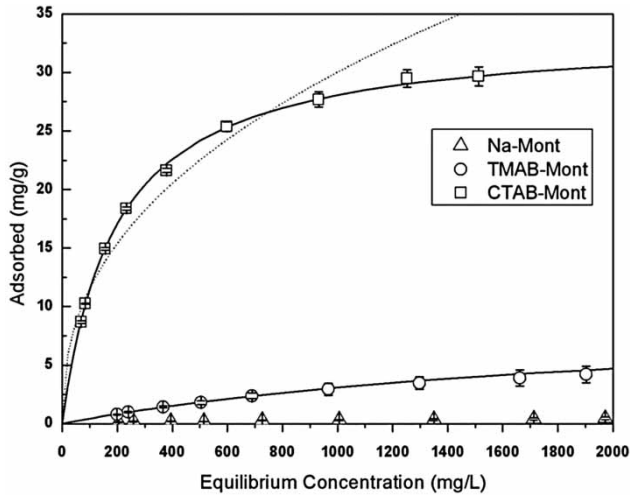

Figure 2 | Contaminant adsorption on Na-Mont (△), TMAB-Mont (○) and CTAB-Mont (□). The solid line is the Langmuir isotherm and dashed line is the Freundlich isotherm.

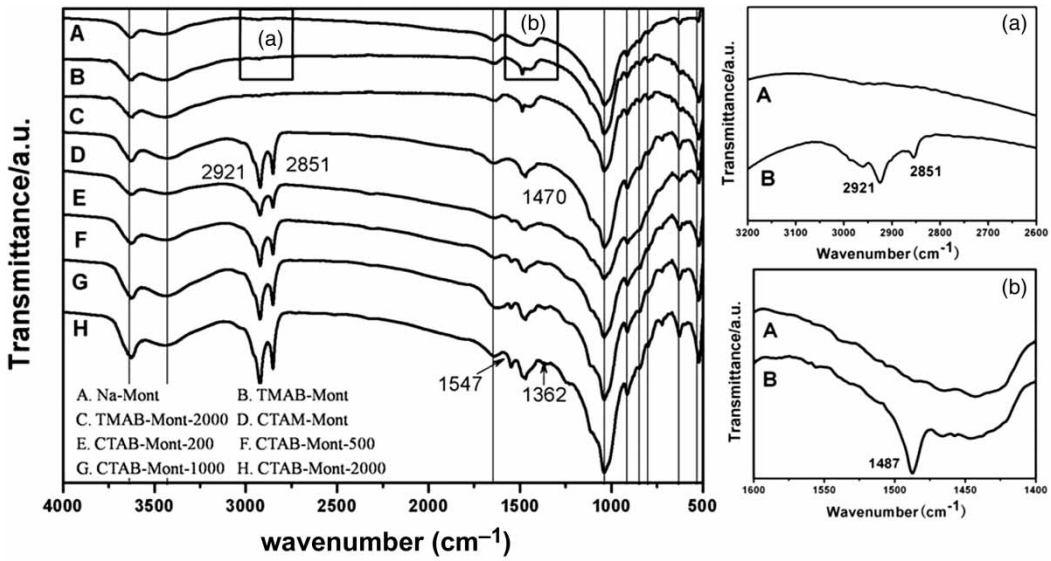

Figure 3 | FT-IR spectra of Na-Mont, TMAB-Mont, CTAB-Mont and contaminant absorbed on TMAB-Mont and CTAB-Mont. Solid vertical lines are peak positions of Na-Mont (Lv *et al*. 2012). Regions (a) and (b) are amplified and shown on the right.

TMAB-Mont. After adsorption in TNT red water, two peaks (1,362 and 1,547 cm^{-1}) appeared on the FT-IR spectrum for CTAB-Mont. These peaks increased in intensity due to N–O symmetric and N–O anti-symmetric stretching, which belonged to the nitro group of DNT-sulfonate. The current results therefore suggested that more contaminants were adsorbed with the increase of COD concentration.

XRD analysis

XRD characterization was performed to describe the expansion of the Na-Mont sheets, which was influenced by the amount and arrangement of QACs. The interlayer spacing and the layer structure of Na-Mont and organic-Monts are depicted in Figure 4. The position of the (001) peaks of organic-Monts were all smaller than that of Na-Mont. The corresponding interlayer spacing increased from 1.28 nm (Na-Mont) to 1.41 nm (TMAB-Mont) and to 2.10 nm (CTAB-Mont). The results indicated clearly that the interlamellar space was expanded after modification and the QACs had got into the interlayer. The differences in interlayer spacings were caused by two effects. Firstly, CTAB is larger than TMAB, and CTAB occupied more space of the interlayer than did TMAB. The other is that the arrangement of TMAB was lateral monolayer, and that of CTAB was lateral bilayer (Lagaly 1981).

After adsorption, the (001) peak of TMAB-Mont was unaffected. But the (001) peak of CTAB-Mont before and after adsorption varied greatly. The (001) peak of CTAB-Mont after adsorption (lines D, E and F) gradually moved to the left as the initial concentration of red water increased. In the curve of F, G, H, the (001) peaks were almost unchanged. This illustrated that with the increase of the initial COD of the red water, the interlayer spacing of CTAB-Mont got larger and more organic contaminants were adsorbed in the interlayer. As the adsorbed organic contaminants reached the capacity of the CTAB-Mont, no more organic contaminants could be adsorbed as further increase of the initial COD of the red water and the interlayer spacing of CTAB-Mont remained the same.

Mechanisms of adsorption

Photographs were taken of samples containing dried CTAB-Mont and TMAB-Mont after adsorption of red water at various COD concentrations. These photos are presented in Figure 5. The samples of TMAB-Mont before and after adsorption had almost no color alteration but the color of CTAB-Mont became redder. The change of sample color corresponded to the increase of the adsorbed organic contaminants.

The mechanisms of the adsorption process were related to the existing states of QACs and the properties of Na-Mont. Na-Mont and TMAB-Mont had almost no adsorption effect on organic contaminants in TNT red water. There was strong electrostatic repulsion between anionic organic contaminants and negative charges to Na-Mont sheets (Jaynes & Boyd 1991), and therefore contaminants could not enter.

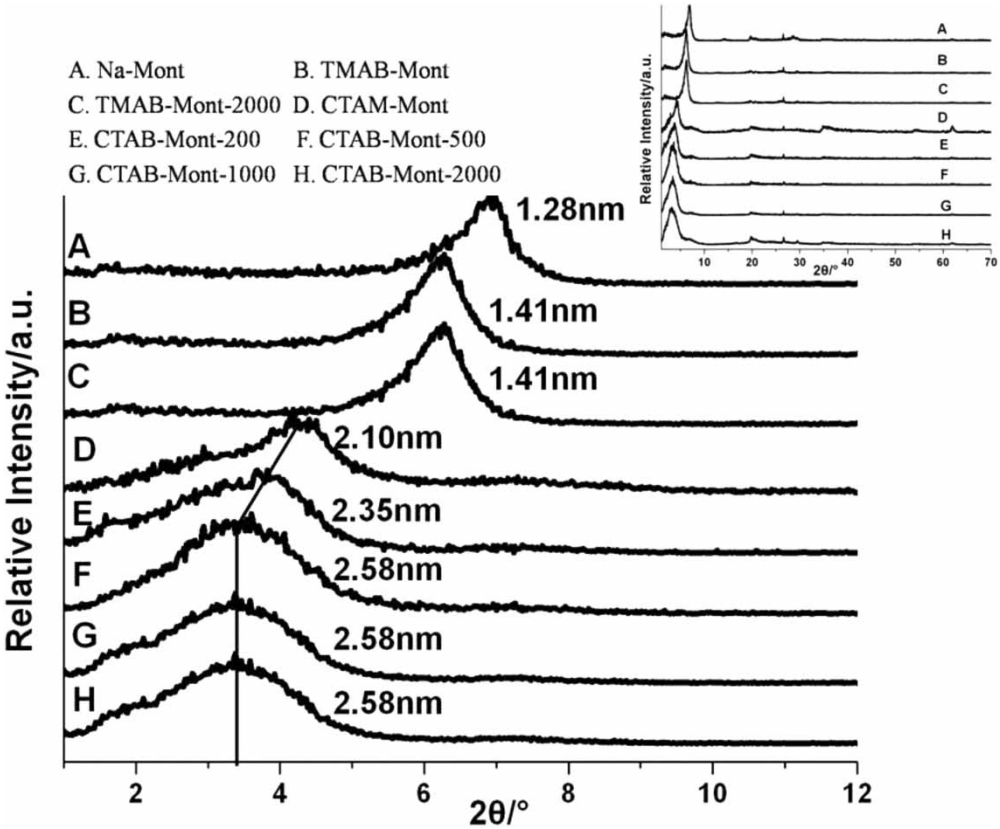

Figure 4 | XRD patterns of samples.

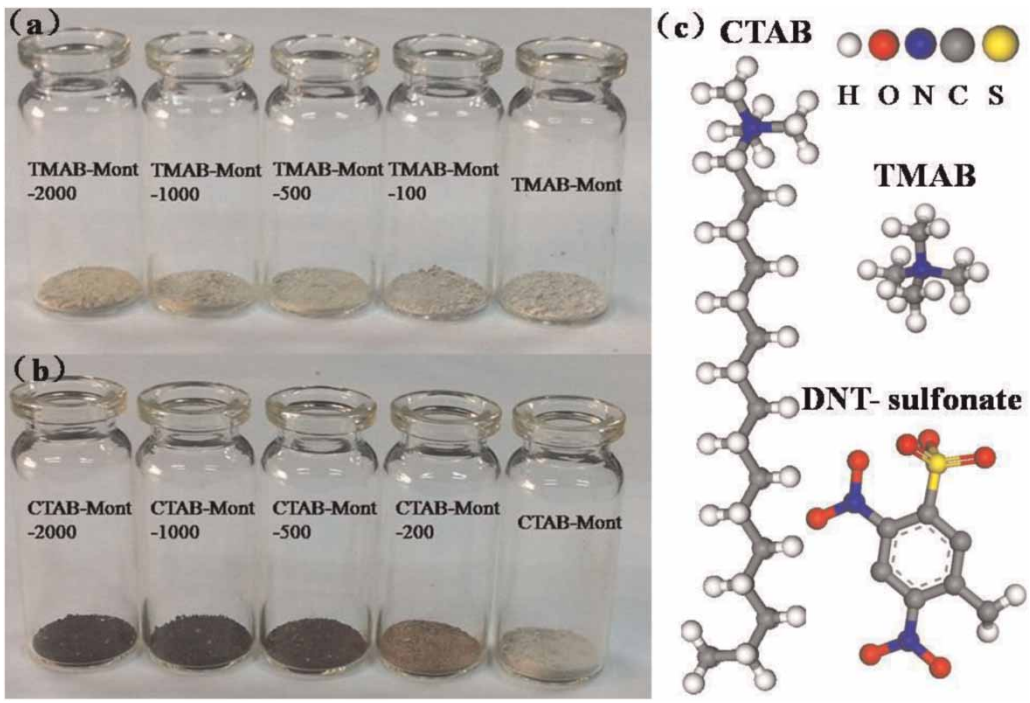

Figure 5 | (a) TMAB-Mont before and after adsorption with different initial COD concentration; (b) CTAB-Mont before and after adsorption with different initial concentration; (c) molecular structure of modification cations and DNT-sulfonate.

CTAB-Mont had a good removal effect of organic contaminants in TNT red water. CTAB greatly increased the interlayer spacing of Na-Mont and promoted the hydrophobicity of CTAB-Mont, ultimately resulting in improved adsorption of pollutants. Compared with TMAB-Mont, the adsorption mechanism of CTAB-Mont was extremely different. The long alkane of CTAB could form an organic phase in the interlayer, while TMAB could not, and the adsorption mechanism of CTAB-Mont towards organic contaminants was the distribution effects between the organic phase and the aqueous solution.

Molecular simulation

Molecular simulation unified the results of XRD and the mechanisms of adsorption, and the results of molecular simulation are shown in Figure 6. Before adsorption, CTAB molecules parallel to each other were arranged as a lateral bilayer in CTAB-Mont. The CTAB in different molecule layers resemble a cross in Figure 6(a). After adsorption, the distribution of pollutants in the interlayer of CTAB-Mont transformed with its concentrations greatly. As the initial COD was 200 mg/L (Figure 6(b)), DNT-sulfonate distributed vertically in the interlayer of

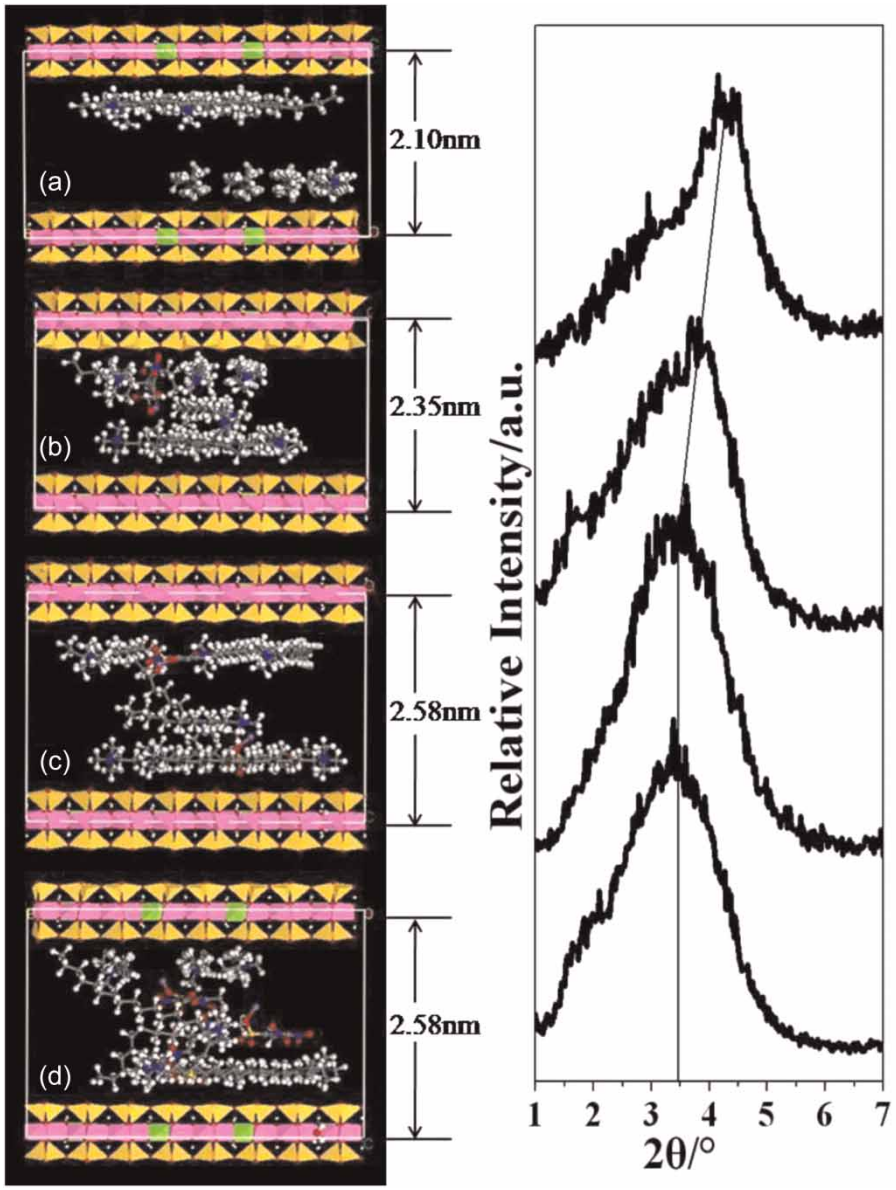

Figure 6 | The left is the result of molecular simulation. The right is corresponding XRD. (a) CTAB-Mont; (b) CTAB-Mont-200; (c) CTAB-Mont-500; (d) CTAB-Mont-2000.

CTAB, and CTAB got closer to the DNT-sulfonate, which had a great expansion effect on the basal spacing of CTAB-Mont. The results corresponded with XRD analysis.

When the COD increased to 500 mg/L, DNT-sulfonate distributed itself parallel to the bi-layer and the arrangement of molecules in the interlayer transferred from two molecular layers to three (Lagaly 1981). DNT-sulfonate turned from vertical into parallel and pushed CTAB out of its own position, making part of the CTAB alkyl chain form a new molecular layer between the former molecule layers after more DNT-sulfonate was adsorbed into the layers due to the steric hindrance as shown in Figure 6(c). The increase of layer spacing was consistent with the results of XRD. When the COD further increased, as shown in Figure 6(d), DNT-sulfonate which was adsorbed later was arranged in the space formed by the former adsorbed molecules. The layer spacing therefore remained constant.

CONCLUSION

Na-Mont and organic-Monts were used as adsorbents of TNT red water. The adsorbents were characterized by XRD and FT-IR. The adsorption effect of CTAB-Mont on organic contaminants in red water was much better than that of TMAB-Mont and Na-Mont. The equilibrium adsorption data were best fitted by the Langmuir isotherm. The adsorption kinetics followed a pseudo-second-order model. The mechanism of organic contaminant adsorption from TNT red water on CTAB-Mont was complex and the distribution phase in the interlayer of Na-Mont was the main factor contributing to the increased adsorption. The results of molecular simulation verified the arrangement of CTAB as well as the organic contaminants (DNT-sulfonate) in the interlayer of Mont and were consistent with XRD results.

ACKNOWLEDGEMENTS

The work was jointly supported by the Fundamental Research Funds for the Central Universities (2652013061 and 2011YXL056) and the Project of Chinese Geological Survey (No. 1212011120309).

REFERENCES

Davel, J., Suidan, M. T. & Adrian, N. 2003 Biodegradation of the energetic compound TNT through a multiple-stage treatment approach. *Water Science and Technology* **49**, 129–135.

Fu, D., Zhang, Y. H., Lv, F. Z., Chu, P. K. & Shang, J. W. 2012 Removal of organic materials from TNT red water by Bamboo Charcoal adsorption. *Chemical Engineering Journal* **193–194**, 39–49.

Jaynes, W. F. & Boyd, S. A. 1991 Hydrophobicity of siloxane surfaces in smectites as revealed by aromatic hydrocarbon adsorption from water. *Clays and Clay Minerals* **39**, 428–436.

Lagaly, G. 1981 Characterization of clays by organic compounds. *Clay Minerals* **16**, 1–21.

Limousin, G., Gaudet, J. P., Charlet, L., Szenknect, S., Barthès, V. & Krimissa, M. 2007 Sorption isotherms: a review on physical bases, modeling and measurement. *Applied Geochemistry* **22**, 249–275.

Liu, N., Wang, M. X., Liu, M. M., Liu, F., Weng, L. P., Koopal, L. K. & Tan, W. F. 2012 Sorption of tetracycline on organo-montmorillonites. *Journal of Hazardous Materials* **225**, 28–35.

Lv, G. C., Li, Z. H., Jiang, W. H., Chang, P. H., Jean, J. S. & Lin, K. H. 2011 Mechanism of acridine orange removal from water by low-charge swelling clays. *Chemical Engineering Journal* **174**, 603–611.

Lv, G. C., Liu, L., Li, Z. H., Liao, L. B. & Liu, M. T. 2012 Probing the interactions between chlorpheniramine and 2:1 phyllosilicates. *Journal of Colloid and Interface Science* **374**, 218–225.

Maloney, S. W., Adrian, N. R. & Hickey, R. F. 2002 Anaerobic treatment of pink water in a fluidized bed reactor containing GAC. *Journal of Hazardous Materials* **92**, 77–88.

Nefso, E. K., Burns, S. E. & McGrath, C. J. 2005 Degradation kinetics of TNT in the presence of six mineral surfaces and ferrous iron. *Journal of Hazardous Materials* **123**, 79–88.

Nehrenheim, E., Odlare, M. & Allard, B. 2011 Retention of 2,4,6-trinitrotoluene and heavy metals from industrial waste water by using the low cost adsorbent pine bark in a batch experiment. *Water Science and Technology* **64**, 2052–2058.

Schmelling, D. C. & Gray, K. A. 1995 Photocatalytic transformation and mineralization of 2,4,6-trinitrotoluene (TNT) in TiO_2 slurries. *Water Research* **29**, 2651–2662.

Wei, F. F., Zhang, Y. H., Lv, F. Z., Chu, P. K. & Ye, Z. F. 2011 Extraction of organic materials from red water by metal-impregnated lignite activated carbon. *Journal of Hazardous Materials* **197**, 352–360.

Wu, Q. F., Li, Z. H., Hong, H. L., Yin, K. & Tie, L. Y. 2010 Adsorption and intercalation of ciprofloxacin on montmorillonite. *Applied Clay Science* **50** (2), 204–211.

Zhou, Y., Kuang, Y., Li, W. Y., Chen, Z. L., Megharaj, M. & Naidu, R. 2013 A combination of bentonite-supported bimetallic Fe/Pd nanoparticles and biodegradation for the remediation of p-chlorophenol in wastewater. *Chemical Engineering Journal* **223**, 68–75.

First received 15 September 2013; accepted in revised form 10 January 2014. Available online 27 January 2014